

MODELING THE MECHANICAL BEHAVIOR OF BUILDING STONES

Ludovico Marques, M. ¹; Chastre, C. ²; Vasconcelos, G. ³

¹ *Barreiro School of Technology, Polytechnic Institute of Setúbal*

² *UNIC, Dept. of Civil Engineering, FCT, Universidade Nova de Lisboa*

ISISE, Dept. of Civil Engineering, Univ. of Minho

ABSTRACT

The building stones assume great importance in building elements of the historical and cultural Portuguese heritage, including sandstone and granite stones. With the aim of evaluating the compressive mechanical behavior of distinct building stones present in the historic built heritage, an experimental research was carried out on selected and representative samples of lithotypes of rocks used in these buildings based on uniaxial compressive tests. Based on experimental results, it was found that porosity plays a central role on the compressive behaviour of granites and sandstones. As porosity can be evaluated in field conditions with non-destructive tests, it was decided to derive an analytical model for the prediction of the compressive behaviour based on the knowledge of porosity of the building stones. For the implementation of the model a cubic polynomial function was adopted for the description of the pre-peak regime under compression. Furthermore, statistical correlation must be defined between mechanical and porosity data. It was observed that good agreement between experimental and analytical stress-strain diagrams, from which the mechanical properties like compressive strength and modulus of elasticity can be derived, was achieved.

KEY WORDS: Built heritage, sandstone, granite, physical and mechanical properties, uniaxial compression, non-destructive tests, analytical model.

1. INTRODUCTION

Portugal is a country where built heritage composed of castles, churches and palaces take an important role in the cultural space. In general, massive masonry walls characterize the construction typology of such ancient constructions and natural stone is the most predominant material. The use of dimension stones in traditional constructions is closely related to the distribution of rock outcrops, being the granitic rocks predominant in the northern and central regions of Portugal, even if it is also possible to find it in some important monuments located in the South. The sandstones have a lesser broad distribution in Portugal, but on a regional scale its use is common in traditional buildings, particularly in the Western regions close to the sea (Peniche, Lourinhã and Silves). Fig. 1 shows some traditional buildings with load bearing masonry from granite and sandstone.

Conservation, rehabilitation and strengthening of the built heritage are clear demands of modern societies, meaning that appropriate intervention techniques on materials and structures should be available. An adequate rehabilitation process of ancient structures should be based on suitable diagnosis and understanding of the existing materials (ICOMOS, 2004) [1]. On the other hand, the principles of safeguarding the architectural heritage according to the international charters of Athens, Venice (ICOMOS, 1965) [2] and Krakow, 2000 [3] recommend that studies should be carried out on the building stone with the lowest degree of intrusion and respect their physical integrity. In fact, one of the main drawbacks in the diagnosis process when an ancient building is being studied is the difficulty of removing material for the mechanical and physical characterization. The principle related to the minimum intrusion has been taken into account broadly by the scientific community that has been proposing alternative non-destructive techniques to evaluate the mechanical and physical properties of construction stone (Popovics, 2003; Malhotra and Carino, 1991) [4, 5]. Ultrasonic pulse velocity (UPV) and Schmidt hammer (rebound number) are two examples of

simple and economical solutions that can give prediction on the elastic mechanical properties and on the weathering state of building stones. Very interesting results were obtained concerning the correlation between UPV and tensile and compressive strength of granites. According to Vasconcelos (2008) [6] UPV has shown to describe the progressive damage on granites under compression at laboratory conditions, which means that it can be used effectively for the damage detection of building stones.

The dependence of the compressive mechanical properties on the physical properties of rocks have been reported by several authors (Goodman, 1989; Palchick, 1999; Hatzor and Palchick, 1997; Tuğrul and Zarif, 1999; Palchick and Hatzor, 2002; Palchick and Hatzor, 2004) [7-12]. The assessment of this relation was also investigated in case of granites, using a set of statistical correlations between mechanical and physical properties (Vasconcelos *et al.*, 2009) [13]. In general, increasing values of porosity are associated to decreasing values of compressive and tensile strength and to the decrease on the modulus of elasticity. This behaviour is to great extent related to the highest heterogeneity and presence of weak bonds in very porous rocks such as pores, voids and microfissures.

The dependence of the basic mechanical properties on the physical properties (porosity) can become the mechanical evaluation of existing building stones of ancient masonry walls much easier. In fact, if porosity is a property that can be easily obtained by Schmidt hammer by ultrasonic pulse velocity (Yasar and Erdoğan, 2004; Vasconcelos, 2005, Vasconcelos *et al.*, 2008) [14-15, 6], the elastic properties can possibly be estimated through the knowledge of the porosity.

Following this idea, a proposal of a model that describe the compressive mechanical behaviour of distinct building stones based on the physical properties has been provided. The analytical model proposed allows the simulation of the compression mechanical behavior of

granite and sandstone in terms of stress-strain relation as a function of physical (porosity) and mechanical parameters (compressive strength and modulus of elasticity).

The implementation of this method involves in a first phase an experimental investigation of the physical and mechanical properties of the building stones under compressive loading (modulus of elasticity and compressive strength). Once the model is defined, it is intended to use it to predict the basic engineering properties based on porosity, which can be given by non-destructive tests.

The major significance of the proposed method is the possibility of gathering enhanced information of the basic engineering properties of ancient building stones by avoiding destructive testing. It should be stressed that compressive strength and modulus of elasticity are the most important mechanical properties enhancing to estimate the masonry compressive strength. Besides, these properties take a major role on the numerical simulation of ancient constructions.

Fig. 1. Traditional buildings with load bearing masonry: (a) vernacular masonry buildings with granite; (b) historical and vernacular construction in sandstone

2. SELECTION OF ROCK LITHOTYPES

The analytical model was developed for sandstones and granites based on the results obtained in the experimental work encompassing mechanical and physical properties of granitic rocks and sandstones.

The granitic stones considered in the present study were mostly collected from the Northern region of Portugal, namely from Afife (AF), Ponte de Lima (PTA), Mondim de Basto (MDB) and Gonça (GA). Mineralogical, textural and structural characteristics were used to select granite types. In this paper only the results obtained on fine to medium and medium granites are reported. The mean length of sections intercepted by a single circle was measured in order to evaluate the grain size of the granitic types, following the principles of the Hilliard single-

circle procedure described in ASTM E112-88 (1995) [16]. Four circles were studied for each granitic facies and sections in the less weathered granitic types were considered. Mean length of sections measured was about 0.5-0.6mm in GA and AF and about 0.7-0.9mm in MDB and PTA lithotypes. The smaller values of grain size were about 0.3mm in GA, MDB and PTA lithotypes, even if the smallest grain size of 0.1mm was recorded in granite AF.

The sandstones were collected in Atougua da Baleia, in Peniche, a region in the Centre of Portugal (Ludovico-Marques, 2008) [17]. Four varieties, which are representative of the two lithotypes in the existing monuments, were identified. It should be noticed that neither coeval quarries nor outcrops of similar materials to those present in the monuments could be found in a close area from Peniche. Thus, stone masonry walls were selected in the vicinity of the built heritage and some samples were extracted from them, taking into account their similarity in terms of visual aspect, mineralogical composition, texture and structure, to the stone existing in the monuments. Additionally, physical tests were carried out to obtain porosity. The four varieties exhibit similar values of porosity to the stone found in the monuments. Both lithotypes have the same classification according to Folk (1974) [18] i.e. they are classified as lithic arkose (Ludovico-Marques, 2008) [17].

The lithotype designated A + B, which includes the varieties A and B, has around 34-40% of carbonates and 30-32% of quartz, whereas the lithotype C+M encompasses typology M which has about 20-21% of carbonates and 45-51% of quartz. The content in carbonates in both lithotypes is so significant such that they were designated by lithic arkose with carbonate cement. In this paper only the results of varieties A, B and M are shown.

The lithotype A + B exhibit macroscopically well-defined lineations and variety A shows clearly visible laminations. Lineations were not detected in variety M. However, in thin sections under polarizing microscope, variety A exhibits one preferred orientation of mica minerals and variety B shows no preferred orientations, being lineations randomly distributed.

Thin sections of variety M show two preferred orientations of mica minerals. All these varieties have about 4-6% of mica minerals.

The average size of grains of quartz and feldspar in the sandstone varieties A and B ranges from 0.1 to 0.13mm, and in variety M the average size is about 0.24mm. Sandstones A and B are, in general, fine-grained whereas variety M have medium to fine grains (Ludovico-Marques, 2008) [17].

The smaller values of grain size in granite lithotypes GA, MDB and PTA are similar to the average size of grains in sandstone variety M. Granite lithotype AF has the smallest values of grain size of four granitic lithotypes studied, which correspond to the average size of grains of sandstone lithotype A+B..

3.EXPERIMENTAL CHARACTERIZATION

The experimental campaign was carried out at laboratory and encompasses uniaxial compression tests to obtain the stress-strain diagrams and the mechanical engineering properties (compressive strength and modulus of elasticity) and porosity tests to obtain physical properties (porosity and density). In this section the details of experimental testing are provided and experimental results are discussed.

3.1.Preparation of samples

The granite lithotypes selected in this study are part of a group that was subjected to extensive experimental research for the mechanical characterization of different types of granite which are typical of most historical and vernacular buildings in the north of Portugal (Vasconcelos, 2005) [15]. For the mechanical characterization of granites it was decided to use cylindrical specimens with a diameter of 75 mm and a height to diameter ratio of approximately two. These dimensions followed the recommendations of ISRM (1981) [19] so that representative samples of the studied granites could be obtained. The granites selected exhibited no very important planar anisotropy. The direction of loading was always in the parallel direction to

the rift plane. With respect to the sandstones, the samples of the three referred varieties were cut into prismatic specimens in order to optimize the scarce rock material available. It was decided to use prismatic specimens of 50x50x100 mm³, corresponding to a height to length ratio of 2. The macroscopic laminations and lineations of lithotype A + B were disposed parallel to the axial length. As in no lineations were detected in variety M, the prismatic specimens were randomly cut (Ludovico-Marques, 2008) [17].

3.2. Study of physical properties

3.2.1. Determination of porosity accessible to water

As aforementioned, the evaluation of the physical properties of rocks can be a simple way to assess the quality of rocks and can assist in the interpretation of the results achieved from mechanical characterization (Goodman, 1989) [7]. Previous studies have shown that the mechanical properties such as compressive strength and elastic modulus are dependent on the porosity and density (Tugrul and Zarif, 1999; Prikiril, 2001; Tugrul, 2004). [10, 20, 21].

The values of porosity and density of the granites were obtained according to the method suggested by ISRM (1981) [19] whereas the porosity and density of the sandstones were obtained following the Recommendations of RILEM (1980) [22] and EN1936 (1999) [23]. Both standards suggest to use vacuum to saturate the specimens. Fig. 2 shows the experimental apparatus. The hydrostatic weighing was carried out after air voids were filled with trapped water. The grain mass, M_s , is defined as the equilibrium mass of the sample after oven drying at a temperature of 105°C. The pore volumes accessible to water were then determined by using the Arquimedes principle allowing to obtain porosity and real densities.

Fig. 2. Testing equipment: (a) glass vessel; (b) specimens container; (c) deionised water reservoir; (d) vacuum pump.

The authors carried out tests to determine other physical properties, such as bulk density, but those results are not presented in the current paper. Additionally, tests were carried out on sandstones to determine the absorption of water at low pressure and by capillarity, as well as to determine the mercury intrusion porosimetry (Ludovico-Marques, 2008) [17].

The porosity tests were carried out in all specimens used in the mechanical characterization to enable a direct correlation between porosity and mechanical properties. The average values of porosity obtained in granites and sandstones are presented in Table 2. It is observed that porosity of the granites ranges from 0.42% (granite GA) to 5.23% (granite MDB). The values obtained to granite MDB are rather high, indicating that this granite is considerably more weathered than the other granites under study, which is denoted macroscopically by the changing of the color and the rough surface. According to Goodman (1989) [7] the expected porosity in fresh granites is lower than 1% but the porosity of igneous rocks tends to increase up to 20% or more as the weathering degree increases.

Table 2. Mean values of physical and mechanical properties of sandstones and granites

The higher porosity of weathered granites can reach values near the lower porosity of sound sandstones. The sandstone samples M exhibit the highest porosity of the varieties studied. In relation to sandstones, it is clear that there is a clear difference in the values of porosity varieties A, B and M ranging from 3.6% to 18.6%. Weathering in sandstones is responsible for higher increase on the values of porosity than in granites, reaching in sandstones values up to 40% close 50% (Palchik, 1999) [8]. This value is very close to the ones pointed out by Tugrul and Zarif (1998) [24] for weathered sandstones.

3.3.Characterization of mechanical behavior

3.3.1.Experimental procedures in monotonic uniaxial compression tests

The experimental campaign on uniaxial compression tests carried out on granites and sandstones was carried out in two Portuguese Universities. The sandstones were tested at laboratory of Structures of New University of Lisbon, whereas the granites were tested at Laboratory of structures of University of Minho.

The uniaxial compression tests on sandstones were carried out in a servo-controlled press Seidner brand, model 3000D, with load capacity up to 3000kN and a piston stroke of 50 mm (Ludovico-Marques, 2008) [17]. The tests were carried out under axial displacement control at a rate of 10 $\mu\text{m/s}$. One LVDT was attached at each side of the specimen between plates of the testing machine. The average displacement was calculated from the displacements measured in the four LVDTs.

In case of granites the uniaxial compression tests were carried out in a stiff prestressed steel frame so that stable response of granite after peak load could be obtained. From a set of preliminary tests it was observed that a very brittle behaviour characterized the behaviour of granites, particularly the fresh granites. The main aim of the extensive experimental work on uniaxial compression tests carried out by Vasconcelos (2005) [15] was the obtainment of the complete behaviour under compression, for which the complete stress-strain diagrams are needed. Thus, the uniaxial compression tests were carried out with circumferential displacement control. For this, a special device using a pantograph was designed to measure the lateral deformations, see Fig. 3. This device is composed by a central ring that is attached locally to the specimen by means of three steel pins. The expansion of the ring is made possible by the lateral spring. The couple of rods attached to the central ring can move freely when the lateral displacement of the specimen increases, since they are connected through an axis. The control LVDT is placed at the end of one of the rods and is able to

measure the deviation between both rods during the compression test. Besides, this device allows the amplification of the actual diametric displacement by a factor of seven, which means that if the programmed velocity of the control LVDT is $2\mu\text{m/s}$, the corresponding lateral increment measured in the specimen is approximately $0.3\mu\text{m/s}$. A set of tests was carried out with uniaxial and circumferential control in weathered granites under uniaxial compression and it was concluded that apart the possibility of obtaining the post-peak behavior no differences were found by using the two distinct deformation control (Vasconcelos, 2005) [15]. The stress-strain diagrams were obtained from the average of three displacements measured by the three LVDTs placed between plates and spaced 120° apart. More details about the experimental procedures can be found in (Vasconcelos, 2005) [15] and (Ludovico-Marques, 2008) [17].

Fig. 3. System used in tests of granite samples to carry out the uniaxial compression tests under the circumferential displacement control

3.3.2. Experimental Mechanical behaviour under uniaxial compression

The mechanical behavior in uniaxial compression of granular rocks can be described through the stress-strain curves encompassing the following stages (Eberhardt et al., 1999; Rocha, 1981) [25, 26] (Fig.4): (i) pre-existing crack closure; (ii) linear elastic deformation; (iii) crack initiation and stable crack growth; (iv) crack damage and unstable crack growth; (v) failure and post peak behaviour. Eberhardt et al. (1999) [25] defined the initial stage of the stress-strain curve as a nonlinear region corresponding to volumetric decreasing due to pre-existing microcracks and voids closure until the stress level σ_{cc} . From this stage, the stress-strain diagram presents a linear stretch corresponding to elastic deformation until the microcracking stress level σ_{ci} . This stress level corresponds to the onset of microcracking. Many previous studies demonstrated that microcracks induced during uniaxial tests are mainly tensile cracks

(Lajtai *et al.*, 1990; Moore and Lockner, 1995; Přikrál *et al.*, 2003) [27, 28, 29]. The shape of the stress-axial strain is not sensitive to this deformational mechanism. This is essentially due to the fact that the compressive stress-parallel cracks do not change the axial stiffness (Li and Lajtai, 1998; Lajtai, 1998) [30, 31].

The unstable microcracking occurs for the crack damage stress level, σ_{cd} , and is associated to the point of reversal in the total volumetric strain diagram. This stage is connected to the maximum compaction of the specimen and to the onset of dilation since the increase on volume generated by the cracking process is larger than the standard volumetric decrease due to the axial load. For this stage, a rapid and significant increase on the lateral strains is observed, as a result of the volume increase. The microcracking spreading is no longer independent, the local stress fields begin to interact and the microcracks previously formed tend to coalesce. After the peak load is reached, the material becomes weaker and the strain is concentrated in the weaker elements (strain localization) which constitute the damaged zone (Vasconcelos, 2005) [15]

Fig. 4. Typical Stress–strain curves

After the peak load is reached, the compressive behavior is characterized by macrocracking growth as strain localization occurs. Macrocracks result from coalescence of the microfractures developed until the peak load is reached. At this stage, the tensile or the shear fractures are fully formed and are visible with naked eye. The strain localization and the growth of the crack length are followed by a significant load carrying capacity decrease of the material, resulting often in the brittle failure of the stone. In general, the post-peak behavior of high strength rocks is hard to be recorded due to its very brittle nature resulting in an abrupt and sudden failure. However, when recorded, the stress-strain diagram drops off abruptly after peak load and softening branch presents distinct negative slopes, being in some

of them even positive (snap-back). In case of low strength rocks, the softening branch is much more smoother. This trend can be seen both in sandstones and granites, see Fig.5 and Fig 6., where the stress-strain diagrams for both types of rocks under analysis are shown. It is observed that in case of low strength sandstones it is possible to capture the post-peak response, whereas the stress-strain diagrams are possible to be recorded only up to peak stress in case of hard sandstones. Vasconcelos et al. (2009) [13] have shown successfully that the post-peak behavior of high strength granites can be recorded easier if the circumferential displacement control was adopted in the compression tests. It is clear that the post-peak behavior of granites is clearly dependent on its strength, similarly to what occurs in sandstones. In fact, in case of high strength granites (GA, PTA) the post-peak presents a sharp decrease on stress for increasing displacements, whereas in case of soft granites (AF and MDB) the post-peak is smooth. In granites GA there are even few abrupt failures after peak load is reached. This behavior appears to be also related to the internal structure of rocks described by the porosity, as it is the result of the internal distribution and arrangement of grains as well as of the internal microfissures, pores and voids.

The evaluation of the post mortem failures of the tested specimens reveals that they appear to be related to weathering state and consequently to the porosity level. In case of fresh granites cracks develop in the subparallel direction to loading, approximately at an angle lower than 10° from the axial longitudinal axis of the specimen. On the other hand, in weathered and high porosity granites the macrocracks localizes within a shear band, see Fig. 7. In case of sandstones, the double shear crack bands appear to be better defined in high porosity sandstones, see Fig. 8. In the sandstone specimens of the lithotype M clear double shear develops, whereas in case of specimens of lithotype A+B (Fig. 8), it is more usual to observe a more distributed subvertical cracks. This can be associated to the existence of microcracks aligned according a preferential plane, as pointed out by Gupta and Rao (2000) [32].

The pre-peak behavior is also dependent on the lithotype. In general, lower strength rocks present also lower values of initial stiffness than high strength rocks, see Fig. 5 and Fig. 6. By comparing the values of compressive strength with the values of porosity, see Table 1, it is evident that the porosity regulates the behavior of rocks in uniaxial compression as it is the result of the distribution and arrangement of grains. It is shown that high porosity granites, which are associated essentially to more weathered levels, present considerably lower stiffness and lower compressive strength. The dependence of the compressive strength and stiffness of sandstones on the porosity follow the same trend as the granites.

Fig. 5. Stress-strain diagrams representing the varieties of sandstones

Fig. 6. Stress-strain diagrams representing the varieties of granites

Fig. 7. Failure modes of granite specimens tested in monotonic uniaxial compression. (a) fresh granites and (b) weathered granites...

Fig. 8 Failure modes of sandstone specimens tested in monotonic uniaxial compression. (a) A variety. (b) B variety. (c) e (d) M variety, front and rear features of specimens.

Both in sandstones and in granites, the strain corresponding to peak stress increases as the compressive strength decreases, which is related to the lower stiffness of low strength granites and sandstones. This means that this parameter is also dependent on the porosity. Increasing values of porosity are associated to increasing deformation at peak stress, see Table 1, confirming that porosity plays a major role on the behavior of rocks under compression.

4. Analytical modelling of the compressive behavior

Given the important role taken by the porosity on the compressive behaviour of rocks, it was decided to find an analytical model that enables to describe compressive behaviour from the knowledge of porosity. As previously mentioned, the porosity of rocks can be easily obtained

through non-destructive tests such ultrasonic pulse velocity (Vasconcelos et al., 2008a) [6] and Schmidt hammer (Vasconcelos, 2005) [15].

The analytical model was developed to sandstones by Ludovico-Marques (2008) [17] and it is applied also to predict the compressive behaviour of granites. As aforementioned, according to Vasconcelos et al. (2009) [13], the mechanical properties of homogeneous granite (without significant planar anisotropy) are also reasonably correlated with porosity.

The value of compressive stress, σ , developed in granites and sandstones can be obtained by Eq. (1):

$$\sigma = f(\varepsilon/\varepsilon_R) \times \sigma_c \quad (1)$$

where σ_c corresponds to the value of compressive strength of rocks and $f(\varepsilon/\varepsilon_R)$ is the shape function characterizing the pre-peak behaviour of rocks under study.

The shape function (f) is obtained by normalizing the compressive stress by the compressive strength, σ_c , and it is dependent on the strain, ε , normalized by the strain at peak strength (ε_R):

$$f(\varepsilon/\varepsilon_R) = \frac{\sigma}{\sigma_c} \quad (2)$$

The calibration of the shape function is performed based on the results of uniaxial compression tests obtained for both types of the rocks considered in this work. Thus, from the analytical expressions of Ludovico-Marques (2008) [17] defined for the sandstones and taking into account the experimental stress-strain diagrams obtained for granites, it is observed that the pre-peak behaviour is well described by a cubic polynomial function. Thus, the shape function valid both for sandstones and granites is given by Eq. (3):

$$f(\varepsilon/\varepsilon_R) = -(\varepsilon/\varepsilon_R)^3 + 1.47(\varepsilon/\varepsilon_R)^2 + 0.5(\varepsilon/\varepsilon_R) \quad (3)$$

The coefficient 1.47 that multiplies the square term in Eq. (3) tends to 1.5, so that the shape function tends to value 1, when the strain tends to ε_R .

Through direct substitution of Eq. (3) in Eq. (1), the compressive stress, σ , is given by:

$$\sigma = \left[-(\varepsilon/\varepsilon_R)^3 + 1.47(\varepsilon/\varepsilon_R)^2 + 0.5(\varepsilon/\varepsilon_R) \right] \times \sigma_c \quad (4)$$

It should be stressed that the model can be easily generalized to other types of rocks because their behavior in the regime of pre-peak is easily adjusted to a cubic polynomial function.

4.2. Correlation between porosity and compressive strength and strain at peak stress

For the implementation of the analytical model aiming at describing the compressive behaviour of distinct types of rocks through porosity statistical correlations need to be found between porosity and experimental compressive strength as well as with the strain at peak stress. Fig. 9 illustrates the variation of uniaxial compressive strength with porosity in the samples of sandstone and granite lithotypes. The regressions that best fit the experimental results listed in Table 1 are set forth as Eq. (5) for sandstones and Eq. (6) for granites:

$$\sigma_c = 206.7e^{-0.129n} \quad (5)$$

$$\sigma_c = 148.8e^{-0.263n} \quad (6)$$

Fig. 9. Relationship between compressive strength (σ_c) and porosity (n) obtained from sandstone and granite samples

In fact, there is a very significant correlation between the compressive strength of sandstones and granites with the porosity, which confirms that this parameter determines the behavior of rocks under compression as was previously discussed. This result is consistent with the correlations found between the compressive strength and porosity by other authors (Prikril, 2001; Tugrul, 2004) [20, 21]. It should be noticed that the porosity may be hindered in the case of granites with high anisotropy due to the fact that the compressive strength varies with the direction of loading and porosity is not clearly a directional property.

Another important parameter for the complete definition of the analytical model is the strain at compressive strength, which can be similarly correlated with the physical properties of materials. Fig. 10 shows the variation of strain at failure (ϵ_R) with porosity in the samples of sandstones and granite lithotypes. As previously mentioned, there is a clear trend for the compressive strain at peak stress to increase as the porosity increase, indicating that high porosity rock are more deformable.

Fig. 10. Relationship between the strain at rupture (ϵ_R) and porosity (n) obtained from sandstone and granite samples

The regressions that best fit the experimental results exhibited in Table 2 are given by Eq. (7) for sandstones and by Eq. (8) for granites:

$$\epsilon_R = 0.0043n^{0.215} \quad (7)$$

$$\epsilon_R = 0.0041n^{0.214} \quad (8)$$

Considering all the specimens of sandstone and granite, the relation between strain at peak stress and porosity is given by granites Eq. (9):

$$\epsilon_R = 0.0042n^{0.222} \quad (9)$$

The better correlation ($r^2=0.942$) found between porosity and strain at peak stress is given for granites by Eq. (8). The correlation between porosity and strain at peak strain found for sandstones is considerably worse. Thus, it was decided to consider for the analytical model the correlation found taking into consideration the results of both rocks under study. Most values of strain at compressive strength (ϵ_R) calculated through Eq. (9) have a variation lower than 10% of experimental values obtained in the sandstone and granite. In granites only specimen GA5 differs 16%. In sandstones the samples AP13, BP13 and MP2 differ 16%, 18% and 19%, respectively.

It is clear that porosity and particularly the distribution of porosimetry influence the compressive mechanical behavior of the material. On one hand, the higher amount of pre-existing microcracks, pores and voids contributes to higher initial deformations corresponding to their closure. On the other hand, the more porous microstructure has higher amount of voids leading to the reduction of the stiffness of the stone skeleton, contributing to the increase on the strain at peak stress. Additionally, rocks with more porous microstructure also show a more remarkable nonlinear behavior in the pre-peak regime, which also contribute to increase the strain at peak stress (Vasconcelos *et al.*, 2008b) [33].

Through the model proposed it is possible to simulate the compressive mechanical behavior of rocks in terms of stress-strain and thereby to obtain the compressive strength and the modulus of elasticity based on the knowledge of porosity. The proposed method has a major significance in terms of practical applications to the study of stone masonry buildings for the estimation of elastic properties, when the extraction of rock core samples is forbidden. Notice that the estimation of the stone mechanical properties is very important when it is needed to assess the stability condition based on numerical simulation or simplified methods.

4.4. Comparison between experimental and analytical results

The analytical model for each stone is completely defined by substituting the compressive strength and strain at peak stress by the expressions found in the previous section that correlate them with porosity. Therefore, it is needed to replace in Eq (4) the compressive strength (σ_c) by Eqs. (5) or (6) for sandstones and granites respectively and the strain at compressive strength (ε_R) by Eq. (9).

The final expression enabling the definition of the stress-strain diagram through the porosity for sandstones is given by Eq. (10):

$$\sigma = 206.7e^{-0.129n} \left\{ -\left(\frac{\varepsilon}{0.0042n^{0.222}}\right)^3 + 1.47\left(\frac{\varepsilon}{0.0042 \cdot n^{0.222}}\right)^2 + 0.5\left(\frac{\varepsilon}{0.0042 \cdot n^{0.222}}\right) \right\} \quad (10)$$

In case of granites the stress-strain diagram can be obtained by Eq. (11):

$$\sigma = 148.8e^{-0.263n} \left\{ -\left(\frac{\varepsilon}{0.0042n^{0.222}}\right)^3 + 1.47\left(\frac{\varepsilon}{0.0042 \cdot n^{0.222}}\right)^2 + 0.5\left(\frac{\varepsilon}{0.0042 \cdot n^{0.222}}\right) \right\} \quad (11)$$

The evaluation of the performance of analytical expression is carried out by comparing the experimental stress-strain diagrams with the ones obtained by Eqs. (10) and (11). From Figs. 11 and 12, when a comparison between experimental and analytical stress-strain diagrams for sandstones and granites respectively is shown, it can be seen that in general good agreement is achieved between experimental and analytical results. It is possible to observe that better agreement is achieved concerning the stiffness in case of sandstones. On the other hand, analytical model is enable to appropriately estimate the compressive strength of granites. This estimation is slightly better than in case of sandstones.

Fig. 11. Analytical modelling of some experimental curves of sandstone samples

Fig. 12. Analytical modelling of some experimental curves of granite samples

5. CONCLUSIONS

This paper presented a general overview of the compressive behaviour of two distinct types of masonry stones, commonly used in ancient masonry buildings with historical value or from vernacular architecture. Besides the experimental details on the uniaxial compressive tests, a discussion of the main results is provided, namely the stress-strain diagrams and the values of the key parameters charactering the pre-peak behaviour, such compressive strength and strain ant peak stress. It was seen that the compressive behaviour is influenced in a great extent by the porosity, which is a property connected to the arrangement of the internal skeleton of stones. More porous rocks have clear lower values of compressive strength and higher strain

at peak stress. The higher porosity revealed also to influence the stiffness (modulus of elasticity) of rocks. Much stiffer rocks are associated to low porosity rocks.

Given this dependency, it was decided to derive an analytical model to describe the compressive mechanical behaviour for sandstones, being the model then extended for granites. This model was defined taking into account the general shape of the pre-peak stress-strain diagrams obtained in the experimental tests and considering that it is well defined by a cubic polynomial function. The polynomial function is dependent on the compressive strength on the strain normalized by the strain at peak stress. The final model for sandstones and granites was stated by considering the statistical correlations found between the compressive strength and strain at peak stress with porosity.

The performance of the analytical model was evaluated by comparing the analytical stress-strain diagrams with the stress-strain diagrams obtained in uniaxial compressive tests. A good agreement between the analytical and experimental results was found, meaning that the compressive behaviour can be well predicted when porosity is known. This procedure has as major advantage in the possibility of estimation the mechanical properties under compression without the use of samples to be tested in destructive conditions.

REFERENCES

- [1] ICOMOS. Recommendations for the analysis, conservation and structural restoration of architectural heritage; 2004.
- [2] ICOMOS. International charter for the conservation and restoration of monuments and sites (the Venice Charter 1964) 1965.
- [3] Krakow Charter. Magazine Trieste Contemporanea, 6/7 2000.
- [4] Popovics, JS. NDE techniques for concrete and masonry structures. Prog Struct Eng Mat. 2003; 5(2):49-59. [5] Malhotra, VM, Carino, NJ. CRC handbook on nondestructive testing of concrete, In: VM Malhotra, NJ Carino editors, Boca Raton: CRC Press. 1991,
- [6] Vasconcelos, G, Lourenço, PB, Alves, CA, Pamplona, J. Ultrasonic evaluation of the physical and mechanical properties of granites". Ultrason 2008a,48(5):453-466..
- [7] Goodman, R. Introduction to rock mechanics. 2nd edition. John Wiley & Sons, Inc., New York 1989.
- [8] Palchik, V. Influence of the porosity and elastic modulus on uniaxial compressive strength in soft brittle porous sandstones. Rock Mech Rock Eng 1999;32(4):303-309.
- [9] Hatzor, YH., Palchick, V. The influence of the grain size and porosity on the crack initiation stress and critical flaw length in dolomites. Int J Rock Mech Min Sci 1997; 34(5):805-816.
- [10] Tugrul, A, Zarif, IH. Correlation of mineralogical and textural characteristics with engineering properties of selected granitic rocks from Turkey. Eng Geol 1999;51:303-317.
- [11] Palchick, V, Hatzor, YH. Crack damage stress as a composite function of porosity and elastic stiffness in dolomites and limestones. Eng Geol 2002;63:233-245.

- [12] Palchick, V, Hatzor, YH. The influence of porosity on tensile and compressive strength of porous chalks, *Rock Mech Rock Eng* 2004;37(4):331-341.
- [13] Vasconcelos, G., Lourenço PB, Alves, AC, Pamplona, J. Compressive behavior of granite: An experimental approach”, *ASCE, J Mat Civ Eng* 2009;21(9): 502-511.
- [14] Yasar, E., Erdoğan, Y. Estimation of rock physicochemical properties using hardness methods, *Engineering Geology*, 2004, 71: 281-288.
- [15] Vasconcelos, G. Experimental Investigations on the mechanics of stone masonry: characterization of ancient granites and behaviour of masonry shear walls. Ph.D. thesis. University of Minho 2005; 266p.
- [16] ASTM E112-88. Standard test method for determining *average grain size*. ASTM 1995.
- [17] Ludovico-Marques, M. Contribution to the knowledge of the effect of crystallization of salts in the weathering of sandstones. Application to the built heritage of Atougua da Baleia. PhD thesis in Geotechnical Engineering, specializing in Rock Mechanics. Universidade Nova de Lisboa. Lisbon 2008, 314p (in Portuguese).
- [18] Folk, R. *Petrology of Sedimentary rocks*. Hemphill Publishing. Austin 1974, 184 pp.
- [19] ISRM Suggested Methods. Suggested methods for determining water content, porosity, density, absorption and related properties and swelling and slake-durability index properties. Brown ET, ISRM. Pergamon, Oxford 1981.
- [20] Příkril, R. Some microstructural aspects of strength variation in rocks. *Int J Rock Mech Min Sci* 2001;38:671-682.
- [21] Tuğrul, A. The effect on pore geometry and compressive strength of selected rock types from Turkey. *Eng Geol* 2004;51:303-317.
- [22] RILEM. Recommended tests to measure the deterioration of stone and to Assess the effectiveness of treatment methods. *Mat Const*, Bourdais-Dunoud 1980; 13(75):175-253.

- [23] EN 1936. Natural stone test method-determination of real density and Apparent density, and of total and open porosity. Eur Stand 1999, 9 pp.
- [24] Tugrul, A, Zarif, IH. The Influence of mineralogical textural and chemical characteristics on the durability of selected sandstones in Istanbul, Turkey. Bulletin of Engineering Geology and Environment, 1998; 57:185-190.
- [25] Eberhardt, E, Stead, D, Stimpson, B. Quantifying progressive pre-peak brittle fracture damage in rock during uniaxial compression. Int J Rock Mech Min Sci 1999;36:361-380.
- [26] Rocha, M 1981. Mecânica das Rochas. Laboratório Nacional de Engenharia Civil. Lisboa 1981, 445 pp.
- [27] Lajtai, EZ, Carter, BJ, Ayari, ML 1990. Criteria for brittle fracture in compression. Eng Fract Mech 1990;37 (1):59-74.
- [28] Moore, DE, Lockner, DA. The role of microcracking in shear-fracture propagation in granites. J Struct Geol 1995;17(1):95-114.
- [29] Příkril, R, Lokajíček, T, Rudajev, V. Acoustic emission characteristics and failure of uniaxially stressed granitic rocks: the effect of rock fabric. Rock Mech Rock Eng 2003;36(4):255-270.
- [30] Li, S, Lajtai, EZ. Modeling the stress-strain diagram for brittle rock loaded in compression. Mech Mat;30:243-251.
- [31] Lajtai, E Z. Microscopic fracture process in a granite. Rock Mech Rock Eng 1998;31(4):237-250.
- [32] Gupta, AS, Rao, KS. Weathering effects on the strength and deformational behavior of crystalline rocks under uniaxial compression state. Eng Geol 2000;56:257-274.
- [33] Vasconcelos, G, Lourenço, PB., Alves, CA, Pamplona, J.. Experimental characterization of tensile strength of granites. Int J Rock Mech Min Sci 2008b;45(2):268-277.

Titles of Figures

Fig. 1. Traditional buildings with loadbearing masonry: (a) vernacular masonry buildings with granite; (b) historical and vernacular construction in sandstone

Fig. 2. Testing equipment for porosity tests: (a) glass vessel; (b) specimens container; (c) deionized water reservoir; (d) vacuum pump.

Fig. 3. Device for the circumferential displacement control in granites

Fig. 4. Stress –strain curves stages

Fig. 5. Stress-strain diagrams representing the varieties of sandstones

Fig. 6. Stress-strain diagrams representing the varieties of granites

Fig. 7. Failure modes of granite specimens tested in monotonic uniaxial compression: (a) fresh granites and (b) weathered granites

Fig. 8. Failure modes of sandstone specimens tested in monotonic uniaxial compression. (a) variety A. (b) variety B. (c) variety M, front and rear features of specimens.

Fig. 9. Relationship between compressive strength (σ_c) and porosity (n) obtained from sandstone and granite samples

Fig. 10. Relationship between the strain at rupture (ϵ_R) and porosity (n) obtained from sandstone and granite samples

Fig. 11. Analytical modelling of some experimental curves of sandstones samples

Fig. 12. Analytical modelling of some experimental curves of granite samples

Tables Titles

Table 1. Mean values of physical and mechanical properties of sandstones and granites

Rock	Sample	σ_c (MPa)	ε_R	n (%)
Sandstone	AP1	102.3	0.00500	4.60
	AP5	105.2	0.0051	4.30
	AP6	104.0	0.00530	4.20
	AP9	120.3	0.0052	4.20
	AP11	136.2	0.00625	3.80
	AP13	135.7	0.00663	3.60
	BP3	95.0	0.00720	7.00
	BP13	105.3	0.00780	6.70
	MP1	18.7	0.00793	18.40
	MP2	20.0	0.00673	18.50
	MP3	24.5	0.00798	17.20
	MP5	17.9	0.00883	18.60
	MP6	17.6	0.00798	18.60
	Granite	GA3	125.3	0.00327
GA5		120.8	0.00301	0.43
GA1		136.2	0.00375	0.45
GA4		137.1	0.00367	0.44
GA2		135.9	0.00351	0.49
GA9		135.4	0.00352	0.48
PTa_15		109.2	0.00430	1.10
PTa_14		111.2	0.00435	1.11
PTa_16		116.0	0.00446	1.11
PTa_13		116.9	0.00443	1.11
AF_L13		68.9	0.00526	2.99
AF_L12		57.7	0.00480	3.04
AF_L8		67.1	0.00559	3.06
AF_L1		66.7	0.00535	3.11
AF_L2		66.1	0.00551	3.19
AF_L11		63.1	0.00536	3.26
MDB_L4		41.1	0.00596	4.77
MDB_L51		39.1	0.00557	4.91
MDB_L61		38.9	0.00582	4.95
MDB_L5		39.1	0.00563	5.14
MDB_L2		41.2	0.00619	5.19
MDB_L71	38.7	0.00562	5.23	



(a)



(b)

Fig. 1. Traditional buildings with load bearing masonry: (a) vernacular masonry buildings with granite; (b) historical and vernacular construction in sandstone



a)



b)



c)



d)

Fig. 2. Testing equipment for porosity tests: a) glass vessel; b) specimens container; c) deionised water reservoir; d) vacuum pump.

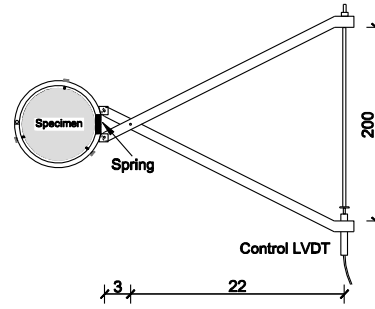
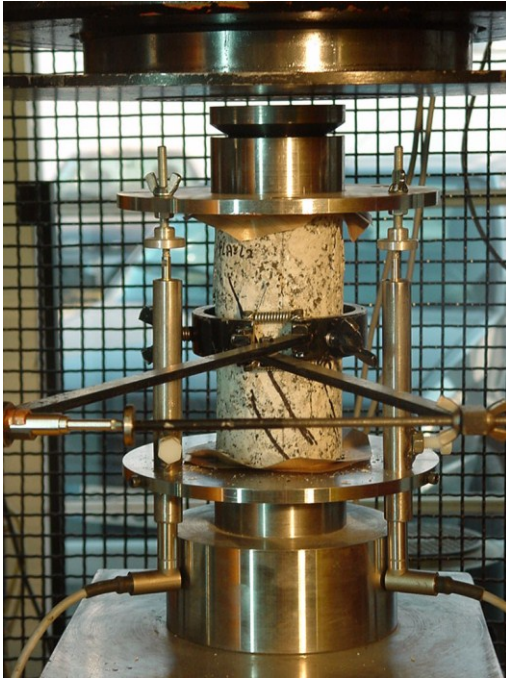
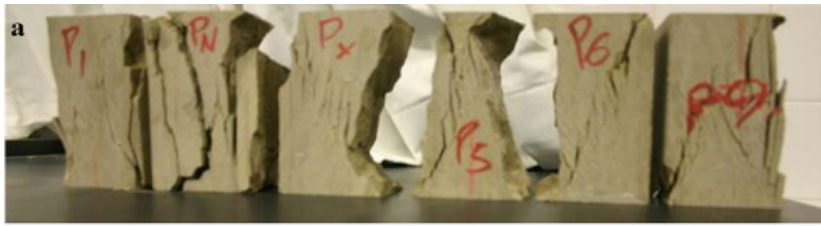
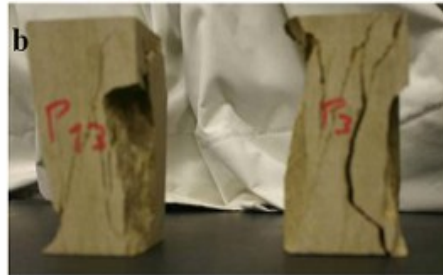


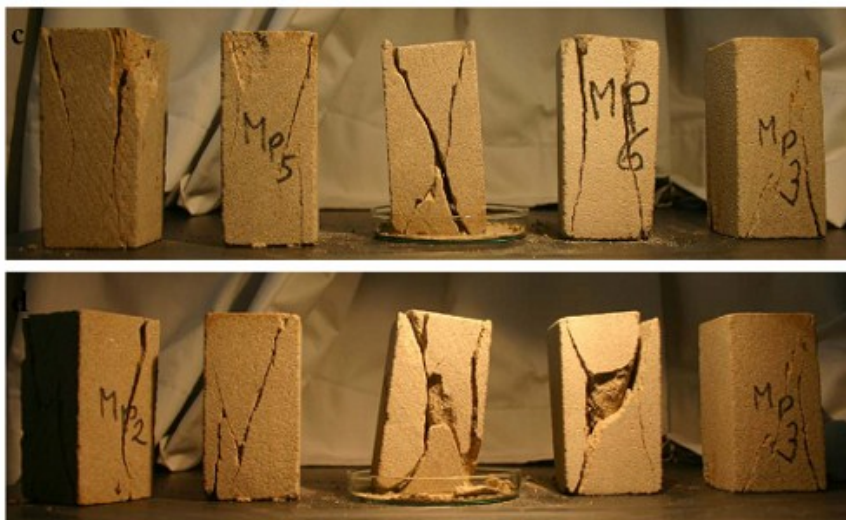
Fig. 3. System used in granite samples to carry out the uniaxial compression tests under the circumferential displacement control



(a)



(b)



(c)

Fig. 8. Failure modes of sandstone specimens tested in monotonic uniaxial compression. (a) variety A. (b) variety B. (c) variety M, front and rear features of specimens.



(a)



(b)

Fig. 7. Failure modes of granite specimens tested in monotonic uniaxial compression: (a) fresh granites and (b) weathered granites

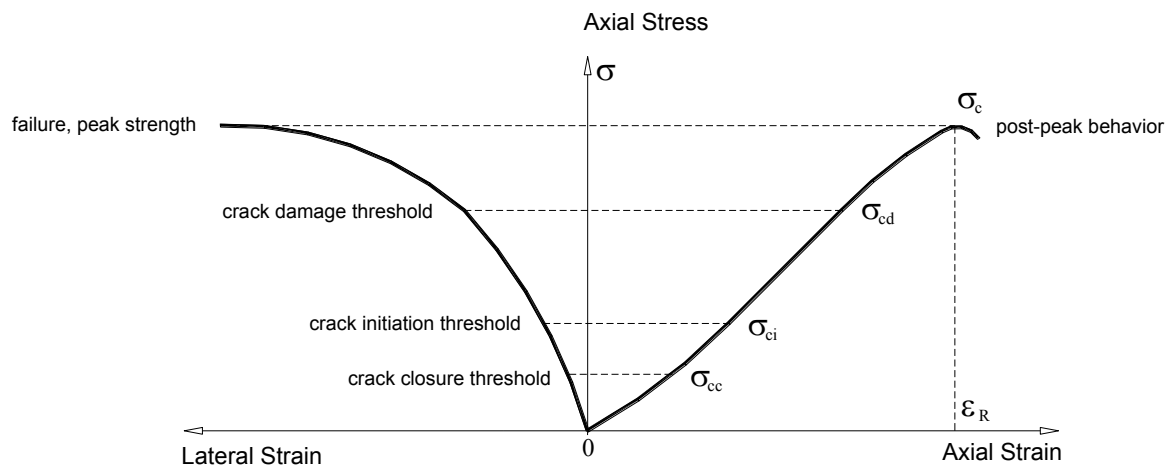


Fig. 4. Stress –strain curves stages

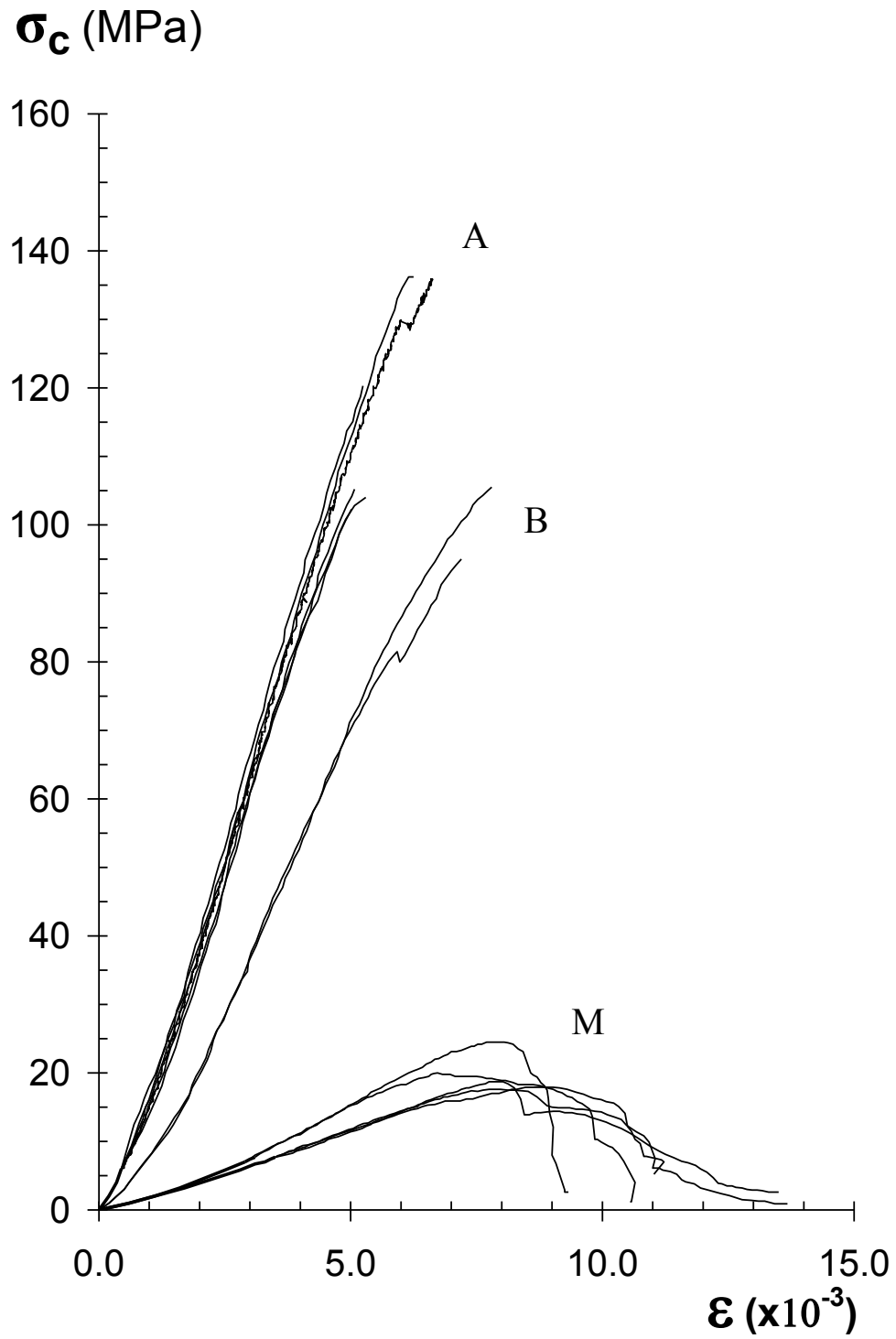


Fig.5. Stress-strain diagrams representing the varieties of sandstones

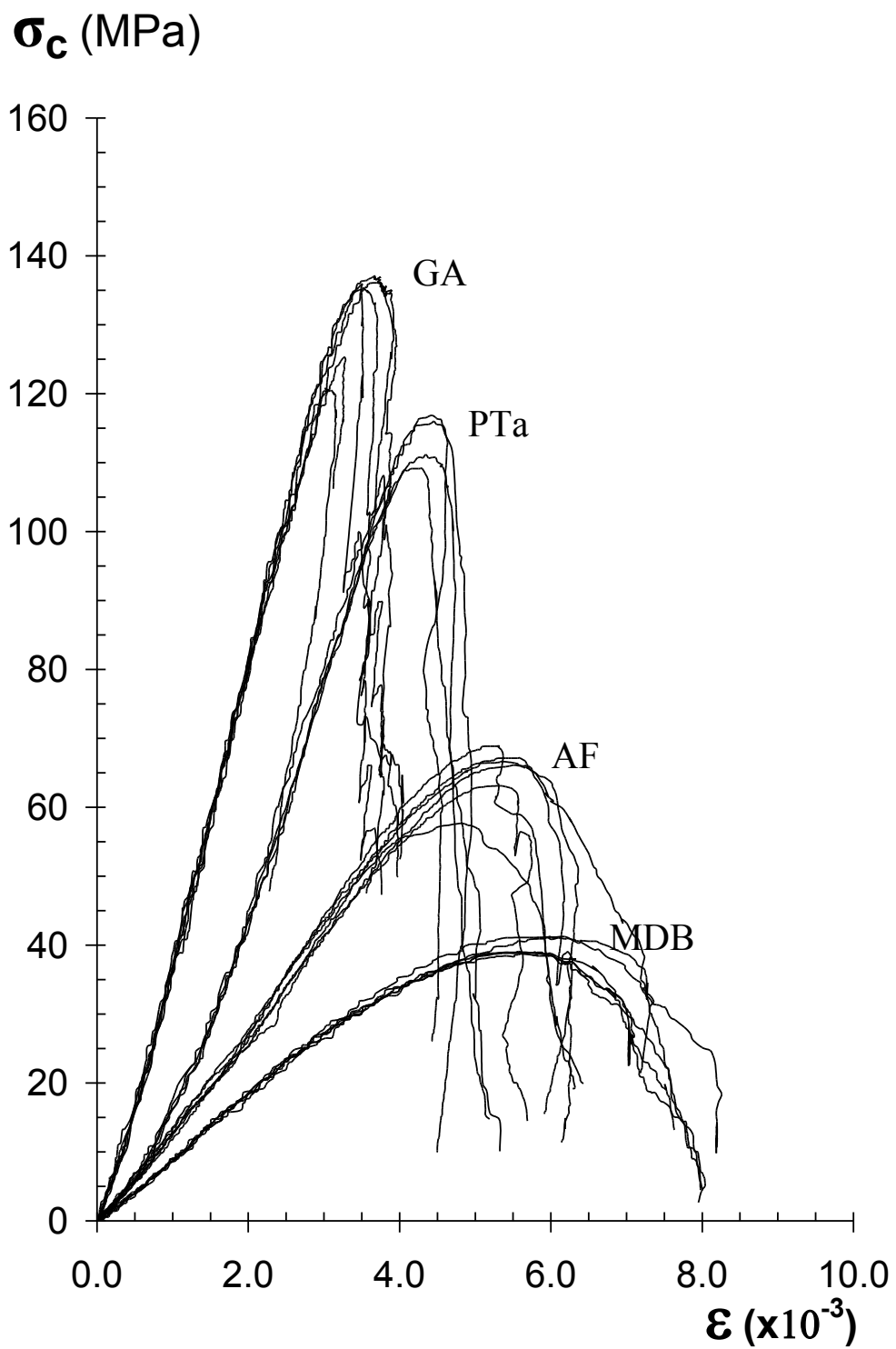


Fig. 6. Stress-strain diagrams representing the varieties of granites

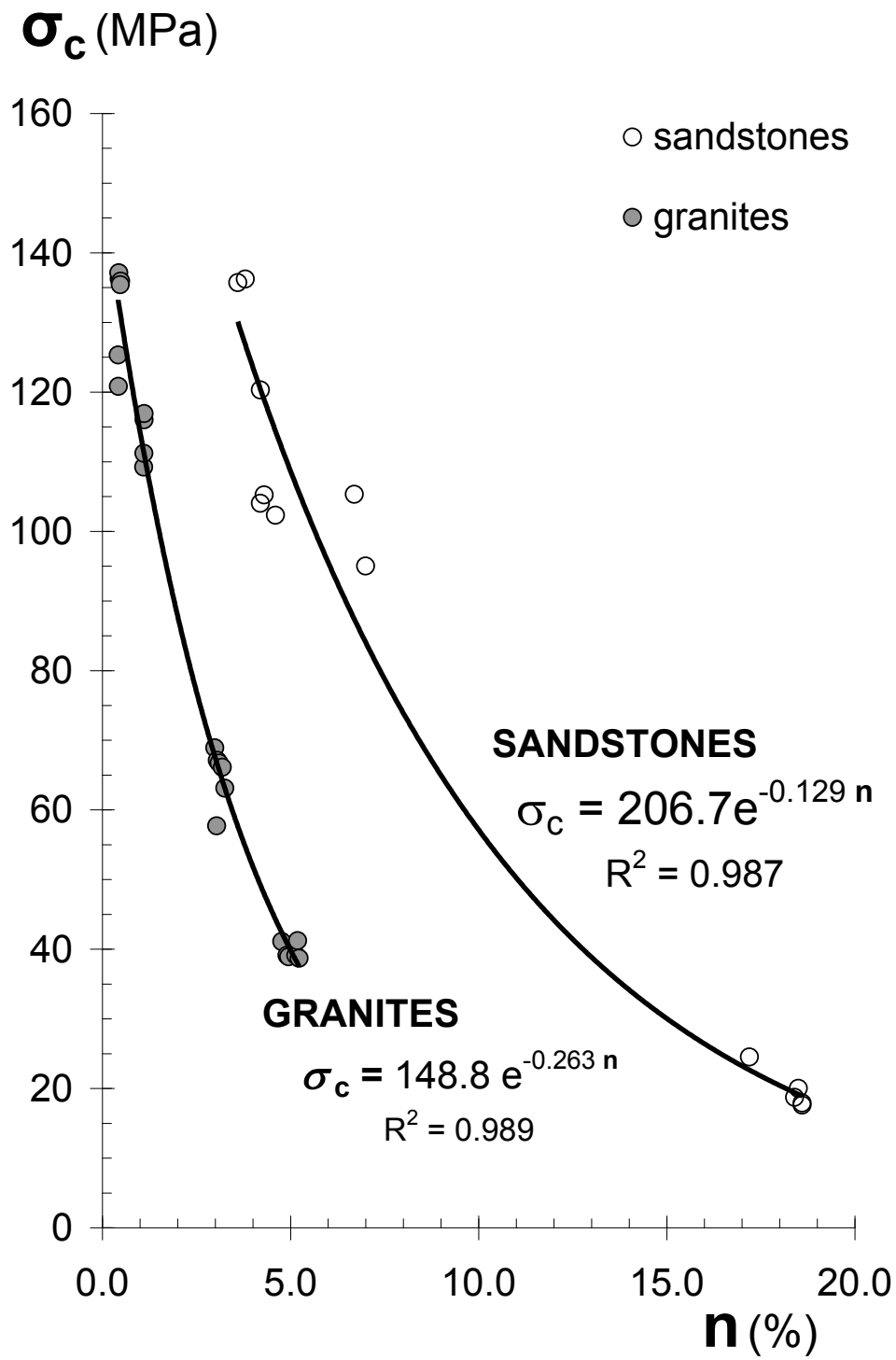


Fig. 9. Relationship between compressive strength (σ_c) and porosity (n) obtained from sandstone and granite samples

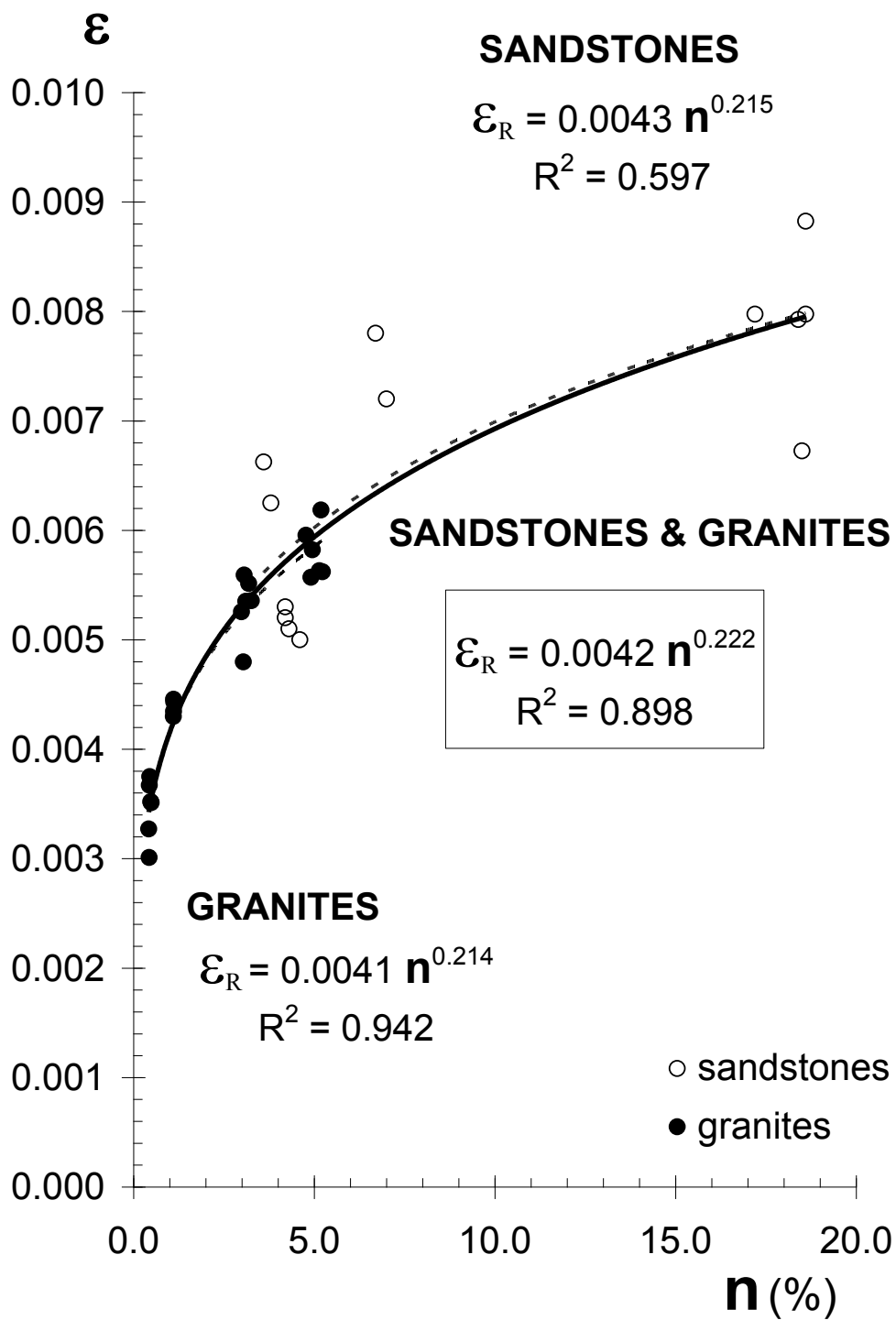


Fig. 10. Relationship between the strain at rupture (ϵ_R) and porosity (n) obtained from sandstone and granite samples

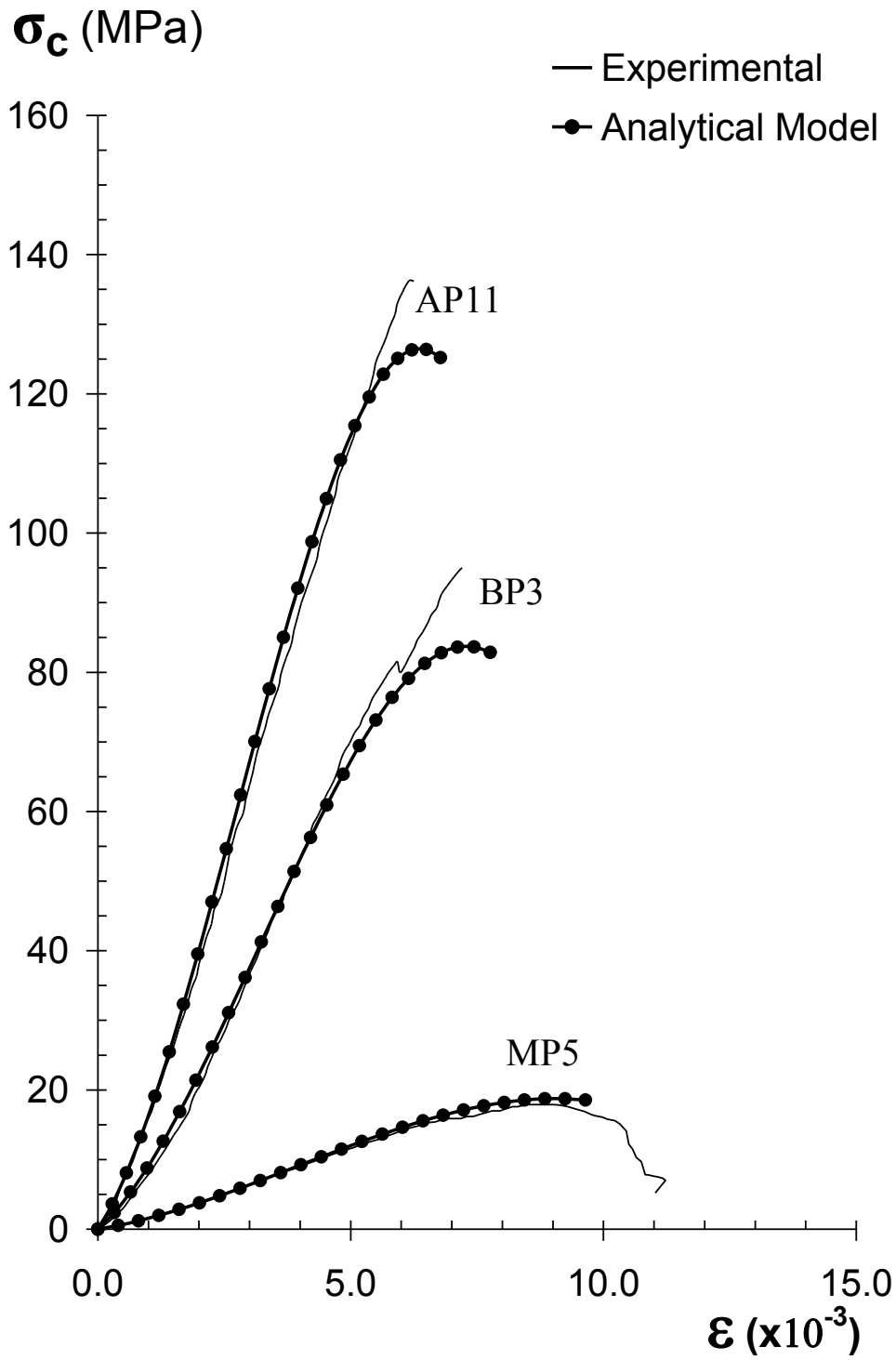


Fig. 11. Analytical modelling of some experimental curves of sandstones samples

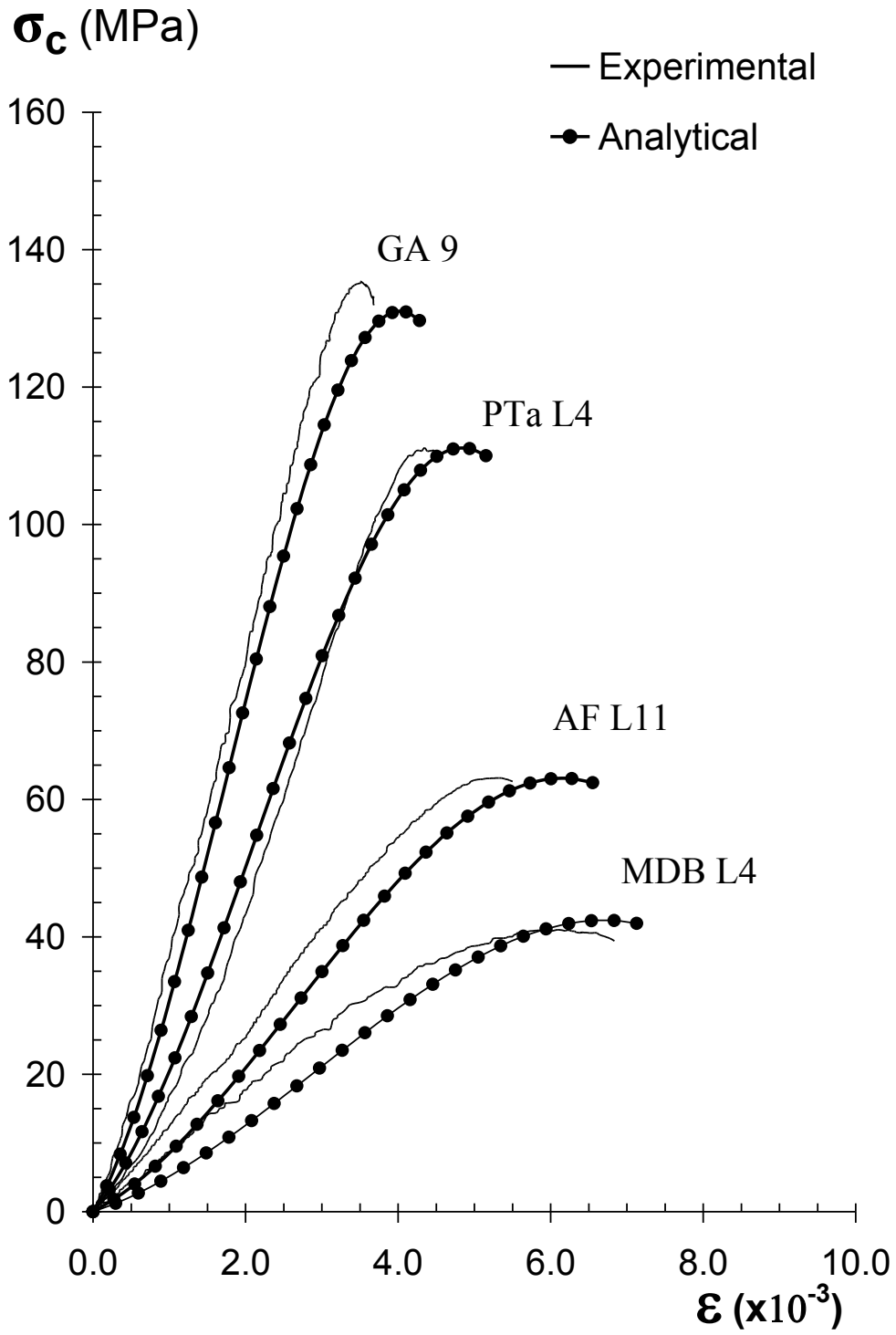


Fig. 12. Analytical modelling of some experimental curves of granite samples